Maximum Efficiency Tuning of Microwave Amplifiers

L. C. Hall and R. J. Trew

High Frequency Electronics Laboratory
Electrical and Computer Engineering Department
North Carolina State University
Raleigh, NC 27695-7911
(919) 737-5248

Abstract

Maximum efficiency tuning conditions for a microwave power amplifier are determined by a statistical impedance matching method. A physics-based MESFET simulator is used to predict optimum device performance. Sensitivity of efficiency to variations in source harmonic impedance matching is described and shown to be significant.

Introduction

High efficiency microwave amplifiers are vital components in phased array radars, mobile communications, and space-technology applications. Higher amplifier efficiency (η) allows smaller and lighter power sources, lower cooling requirements, and enhanced reliability.

Achievements in high efficiency amplifier design include:

- 1981 $\eta_{pa} = 72\%$ f=2.4GHz $P_{out} = 1.2W$ Gain=8.0dB [1]
- 1982 $\eta_{pa} = 38\%$ f=9.5GHz $P_{out} = 0.7W$ Gain=4.5dB [2]
- 1986 $\eta_{pa} = 45\%$ f=1.0GHz $P_{out} = 1.0W$ Gain=5.8dB [3]
- 1987 $\eta_{pa} = 75\%$ f=1.7GHz $P_{out} = 2.7W$ Gain=9.0dB [4]
- 1988 $\eta_{pa} = 70\%$ f=2.0GHz $P_{out} = 5.0W$ Gain=9.0dB [5]
- 1989 $\eta_{pa} = 36\%$ f=5.5GHz $P_{out} = 1.5W$ Gain=5.0dB [6]
- 1990 $\eta_{pa} = 61\%$ f=10GHz $P_{out} = 0.45W$ Gain=7.0dB [7]

In this work a harmonic balance microwave simulator which employs a physics-based model for the MESFET is used to investigate RF circuit tuning conditions that result in maximized power-added efficiency (η_{pa}) for a GaAs single-MESFET power amplifier. Previous investigations of high efficiency tuning were based upon Fourier series analysis of ideal terminal waveforms. For this study, no a priori assumptions of ideal input and output loading conditions are made. Circuit impedances at the fundamental and harmonic frequencies that must be presented to the device at both the output and input ports are determined by means of a stochastic optimization technique. Simulations indicate that proper harmonic tuning can achieve $\eta_{pa} \approx 80\%$ at 5GHz.

Power-added efficiency is defined as $\eta_{pa} = \frac{P_{out}-P_{in}}{P_{dc}} \times 100$ This definition of efficiency is preferred over others because it takes the source fundamental conjugate match into account, and therefore provides more realistic estimates of amplifier performance. Other efficiency definitions, such as drain efficiency ($\eta_d = \frac{P_{out}}{P_{dc}} \times 100$), are useful but do not provide as much information as η_{pa}.

Amplifier Classes

Class A amplifiers offer linear operation and low signal distortion at the expense of optimal efficiency. Class B and C amplifiers address the problem of low efficiency by operating at a bias point near pinchoff so that minimum DC power is dissipated. Ideal high efficiency operation occurs when the harmonics of the output voltage have the right magnitudes and phases to form a square wave[8] (Figure 1). This condition can be approximated by placing short circuits at the even harmonics and open circuits at the odd harmonics[9].

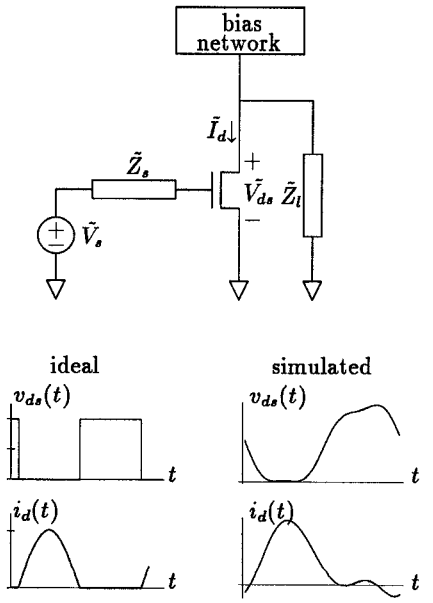

Figure 1: Amplifier Topology and Output Waveforms

CH2870-4/91/0000-0123$01.00 © 1991 IEEE

Class B amplifiers are typically impedance matched at the source and load fundamental, but the harmonic terminations are often formed by capacitive shunts. From ideal waveform analysis, the maximum theoretical efficiency of class B amplifiers is 78%, compared to 50% available from class A circuits[1].

Class C amplifiers are harmonically tuned at the load. Since the ideal square wave output voltage contains only odd harmonics, it is desirable to reflect all even harmonic energy back into the device with 180° phase shift so that even harmonic cancellation occurs. The impedance of the load 2nd harmonic of class C amplifiers is adjusted to achieve this reflection with series resonance, but the source 2nd harmonic impedance is not tuned. The maximum theoretical efficiency of class C amplifers is 100%, although this condition occurs at zero output power.

Higher efficiency occurs at lower output power for class C amplifiers because much of the spectral energy of the ideal output voltage and current waveforms is contained in higher order harmonics which cannot be matched with current technology. The harmonic distribution of energy is such that higher voltages and lower currents produce higher efficiencies at lower output powers (Figure 2).

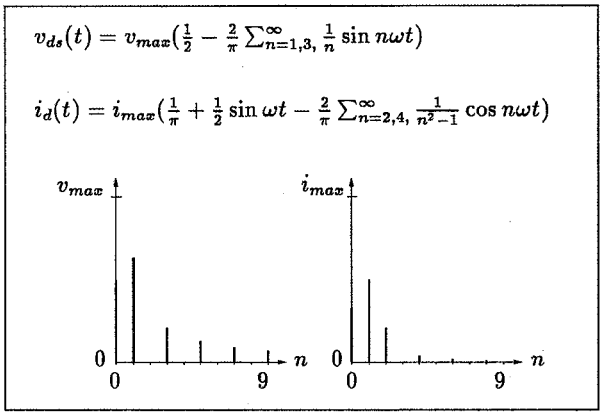

Figure 2: Harmonic Spectrum of Ideal Output Waveforms

Optimization of η_{pa}

A physics-based MESFET simulator, TEFLON [10], was used to investigate the effect of circuit tuning on an amplifer's η_{pa}. Mathematica and Unix scripts were used to collect and plot the data from TEFLON. For a given set of harmonic impedance values, TEFLON can sweep input power to find the input power level which provides the highest efficiency in about one minute of workstation cpu time. A novel technique was employed in which random impedance values for the input and output matching circuits were selected and simulated. After a sufficient number of simulations had been accumulated the result was an unbiased, statistically pure survey of the 12 dimensional space which describes the problem.

The transistor model used for the simulation was an ion-implanted device with a gate length of 0.5μm, a gate width of 1250μm, and a peak doping of $1.6 * 10^{17}\text{cm}^{-3}$. These values are from an experimental transistor which was designed for good efficiency. The simulated and measured RF performance at 5.5GHz for this device before matching circuit optimization are shown in Figure 3. These results employed conjugate impedance matching on the input and output at the fundamental and untuned 2nd harmonic shorts on the input and output. As indicated, maximum η_{pa} obtained with this simple matching circuit is about 50%.

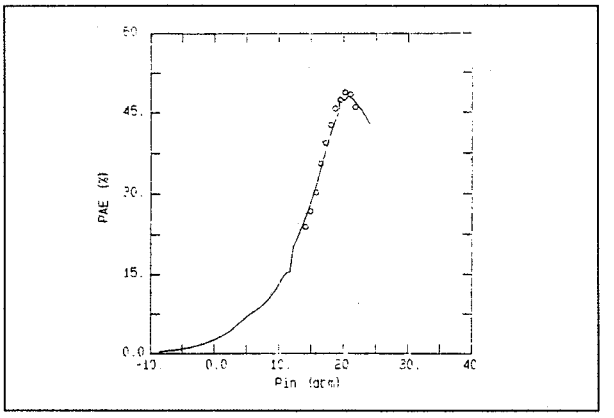

Figure 3: Measured and Simulated η_{pa} Before Optimization

The probability of finding a good combination of the 12 impedance variables is extremely low. For example, if 10% of the guessed region for each variable is considered to be near the $\eta_{pa_{max}}$ point in the 12d space, then the probability that a given guess will have all 12 variables in that region is 10^{-12}. Fortunately, 4 of the 12 variables were found to have comparatively flat response surfaces, and the interdependence of the variables is not very large.

The initial data set provided only subtle trends in the most sensitive variables: the source and load fundamental impedances. These mild trends gave enough information to constrain the range of the source and load fundamental variables. Hence, the next set of simulations was performed in a region of the original impedance hyperbox which was statistically likely to contain the $\eta_{pa_{max}}$ point.

Figure 4 shows some selected plots of the random data from various stages in the optimization. In the leftmost plot of Figure 4, all resistance and reactance variables have been randomly selected from the range $0\Omega \leq R \leq 100\Omega$ and $-100\Omega \leq X \leq 100\Omega$. All combinations of impedances in this first data set achieve η_{pa} below 60%. The peak seen at the top of the leftmost plot indicates a trend in the source fundamental reactance variable which suggests that the optimum combination of impedances has a value of X_{s_1} in the range $0\Omega \leq X_{s_1} \leq 50\Omega$.

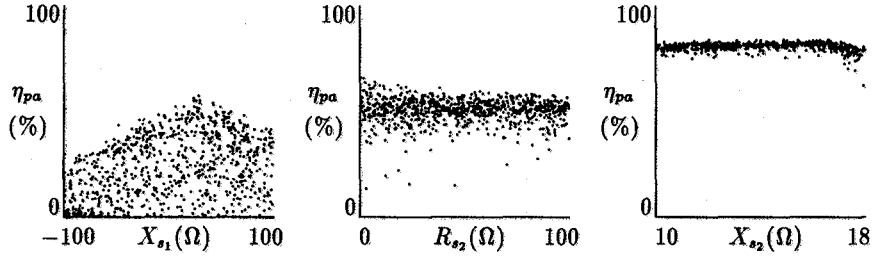

Figure 4: Selected Scatter Plots of η_{pa} Optimization

	source	load
fundamental	$16.0 + j28.0$	$50 + j13.5$
2nd harmonic	$0.0 + j16.0$	$0.0 - j4.0$
3rd harmonic	large	large

Figure 5: Impedances at $\eta_{pa_{max}}$

The center plot of Figure 4 shows the source 2nd harmonic resistance from the third data set of the optimization. The upper edge of this plot has a subtle trend which suggests that lower values of R_{s_2} will correspond to higher efficiency. In fact, $R_{s_2} = 0$ later proves to be a necessary condition for $\eta_{pa_{max}}$.

In the rightmost plot of Figure 4, all impedance variables have been optimized to their best or near-best values. The harmonic impedance values which correspond to the $\eta_{pa_{max}}$ point are shown in Figure 5.

Figure 6 shows the calculated η_{pa}, output power, and gain as a function of input power for the best combination of impedances. The device simulations predict 28.4dBm output power at 10.4dB gain with $\eta_{pa} = 80.5\%$ and $\eta_d = 88.7\%$ when driven by an 18dBm input signal at 5GHz.

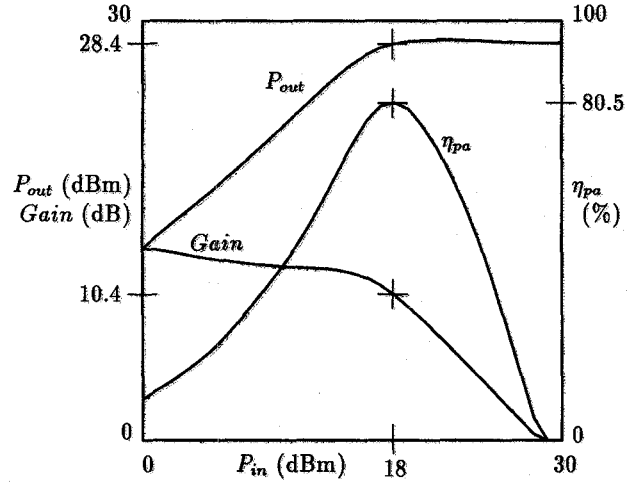

Figure 6: Simulation Results at $\eta_{pa_{max}}$

Characterization

Once the optimum impedances were found, the sensitivity of η_{pa} to changes in each variable was examined. This was accomplished by sweeping each impedance within a 100Ω range and plotting the resulting η_{pa} surface.

Figure 7 shows contour plots of the variation of η_{pa} with impedance near the $\eta_{pa_{max}}$ point. Note that these plots do not represent the entire 12d space because 10 variables were held at their best values for each plot. Though further characterization is needed, the plots in Figure 7 can be used as general guidelines when matching a device for high η_{pa}.

This study demonstrates the importance of source harmonic tuning. The source 2nd harmonic contour of Figure 7 shows that changes in the source 2nd harmonic impedance can vary the η_{pa} from 30% to 80%. The resonant effect also occurs at the load 2nd harmonic.

The 3rd harmonic contours of Figure 7 indicate that η_{pa} is relatively insensitive to third harmonic impedance. However, certain values of third harmonic impedance can lower η_{pa} from 80% to 55%.

By modeling the MESFET as a Thevenin source, the dependence of η_{pa} on the second harmonic impedances can be described as a linear function of the phase shift of the Thevenin source's output voltage. The MESFET can be modeled as a Thevenin equivalent source with voltage $\tilde{V}_{Th}$ and impedance $\tilde{Z}_{Th}$. Correspondingly, the load can be modeled with impedance $\tilde{Z}_2$, and output voltage $\tilde{V}_2$. For this model, phase shift of the output voltage with respect to the Thevenin voltage can be plotted as a function of $\tilde{Z}_2$.

$$\phi\left(\frac{\tilde{V}_2}{\tilde{V}_{Th}}\right) = \arctan\left(\frac{R_{Th}X_2 - R_2X_{Th}}{R_2(R_2 + R_{Th}) + X_2(X_2 - X_{Th})}\right)$$

$$\eta_{pa}(R_2, X_2) = m\phi\left(\frac{\tilde{V}_2}{\tilde{V}_{Th}}\right) + \eta_{pa_0}$$

The resulting surface has the same characteristic shape that η_{pa} has when plotted as a function of $\tilde{Z}_{s2}$ or $\tilde{Z}_{l2}$. If appropriate values of m, η_{pa_0}, R_{Th} and X_{Th} are determined, then the above function $\eta_{pa}(R_2, X_2)$ will very closely match the second harmonic contours shown in Figure 7.

Conclusion

Previous work by others in high efficiency amplifier design has proven that power-added efficiencies as high as 75% can be achieved at microwave frequencies. This has been accomplished mostly by adjusting the input and output biases, conjugate matching the input and output fundamental impedances, and controlling the output second harmonic impedances or signals in creative ways. This work shows that it is also necessary to control the input second harmonic impedance in order to obtain the best possible efficiency. For a single MESFET amplifier, both the input and output second harmonic impedances should be adjusted so that series resonance occurs.

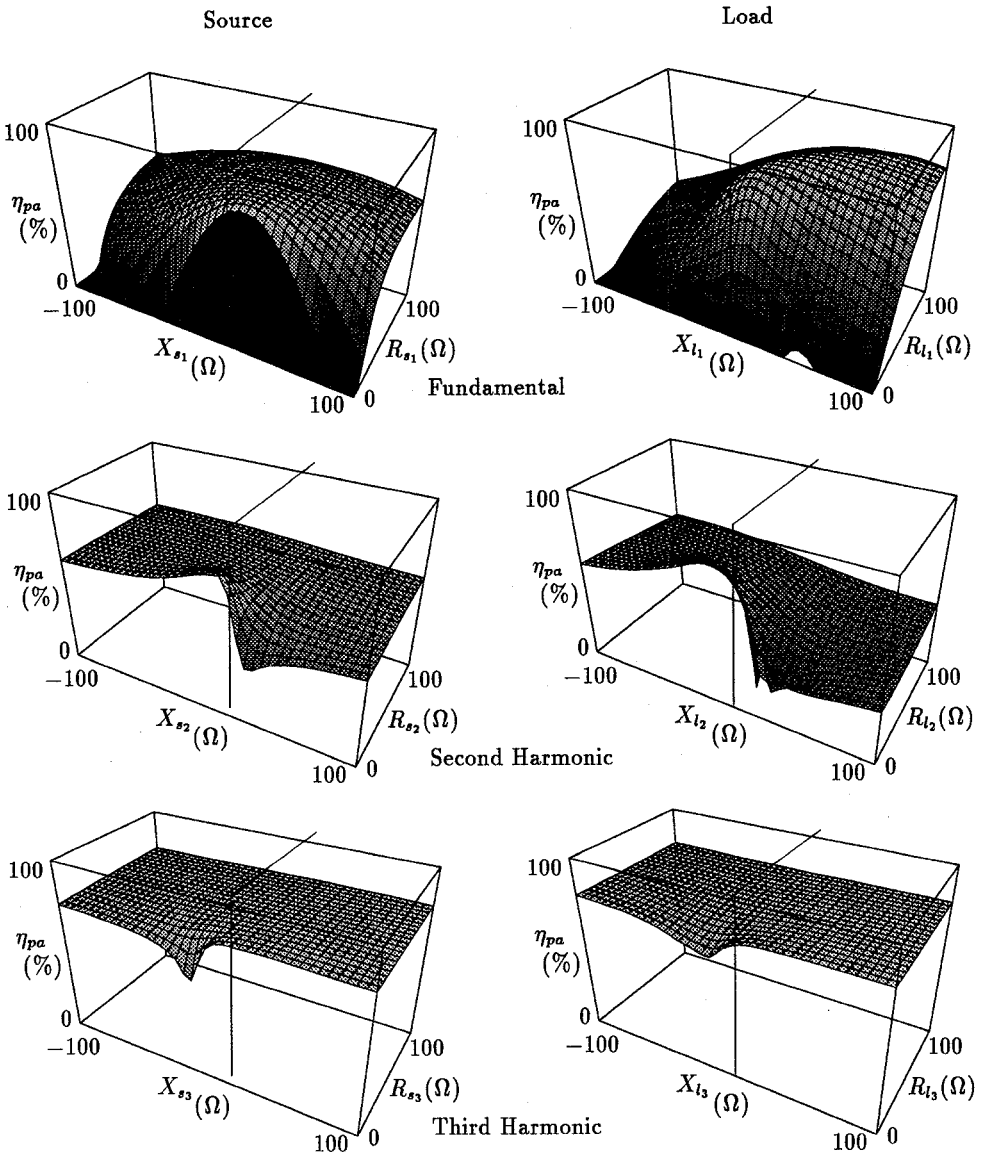

Figure 7: Sensitivity of η_{pa} to Harmonic Impedances

References

1. F. N. Sechi, "High Efficiency Microwave FET Power Amplifiers", Microwave Journal, pp 59-62+, 1981.

2. M. Cohn, J. E. Degenford, and R. G. Freitag, "Class B Operation of Micrwave FETs for Array Module Applications", IEEE MTT-S Digest, pp 169-171, 1982.

3. J. R. Lane, R. G. Frietag, H. Hahn, J. E. Degenford, and M. Cohn, "High-Efficiency 1-, 2-, and 4-W Class-B FET Power Amplifiers", IEEE Transactions on Microwave Theory and Techniques, Vol. MTT-34, No. 12, December 1986.

4. S. Nishiki and T. Nojima, "Harmonic Reaction Amplifier - A Novel High-Efficiency and High-Power Microwave Amplifier", IEEE MTT-S International Symposium Digest, pp 963-966, 1987.

5. T. Nojima and S. Nishiki, "High Efficiency Microwave Harmonic Reaction Amplifier", IEEE MTT-S International Symposium Digest, pp 1007-1010, 1988.

6. I. J. Bahl, E. L. Griffin, A. E. Geissberger, C. Andricos, and T. F. Brukiewa, "Class-B Power MmIC Amplifiers with 70 Percent Power-Added Efficiency", IEEE Transactions on Microwave Theory and Techniques, Vol. 37, No. 9, September 1989.

7. M. A. Khatibzadeh and H. Q. Tserng, "Harmonic Tuning of Power FETs at X-Band", IEEE MTT-S International Symposium Digest, 1990.

8. D. M. Snider, "A Theoretical Analysis and Experimental Confirmation of the Optimally Loaded and Overdriven RF Power Amplifier" IEEE Transactions on Electron Devices, December 1967.

9. H. L. Krauss, C. W. Bostian, F. H. Raab, *Solid State Radio Engineering*, 1980.

10. M. Ali Katibzadeh and Robert J. Trew, "Large-Signal, Analytic Model for the GaAs MESFET", IEEE Transactions on Microwave Theory and Techniques, Vol. 36, No. 2, February 1988.